

**Inflammatory Cell Induced Corrosion in Total Knee Arthroplasty:
A Retrieval Study**

Arianna Cerquiglini¹, Johann Henckel¹, Harry Hothi¹, Anna Di Laura¹, John Skinner¹, Alister J. Hart¹

1. Institute of Orthopaedics and Musculoskeletal Science, University College London
and the Royal National Orthopaedic Hospital, Stanmore, United Kingdom

Corresponding Author:

Arianna Cerquiglini

Institute of Orthopaedics and Musculoskeletal Science (University College London)

Royal National Orthopaedic Hospital, Brockley Hill, Stanmore

Middlesex, HA7 4LP, United Kingdom,

Phone: +44 (0) 208 909 5825, Fax: +44 (0) 208 954 8560

Email: arianna.cerquiglini.15@ucl.ac.uk

We declare that all authors listed have participated in the research and that this article has not been submitted elsewhere. We confirm that all investigations were conducted in conformity with ethical principles of research, that informed consent for participation in the study was obtained and that institutional approval of the human protocol for this investigation was obtained.

Two authors received funding from the British Orthopaedic Association through an industry consortium of nine manufacturers: DePuy International Ltd, Zimmer GmbH, Smith & Nephew UK Ltd, Biomet UK Ltd, JRI Ltd, Finsbury Orthopaedics Ltd, Corin Group PLC, Mathys Orthopaedics Ltd, and Stryker UK Ltd.

Abstract

Metal release in patients with joint replacements is associated with local tissue reactions, pain and ultimately revision of implants. One of the causes of this metal loss is speculated to be due to a mechanism of inflammatory cell induced corrosion (ICIC).

In this knee retrieval study, we aimed to: (1) identify the extent and location of ICI corrosion patterns on our femoral and tibial components and (2) correlate our findings with implant and clinical information. We investigated 28 femoral and 9 tibial components made of polished CoCr for presence of ICIC, using macroscopic and microscopic screening and statistical analyses to identify any significant correlations between our results and clinical information.

We found that 71% of femoral and 100% of tibial components showed evidence of ICIC and significantly more was present on non-contacting regions ($p < 0.0001$). We found a significant correlation between the presence of ICIC and instability ($p = 0.0113$) and a significant difference between poster stabilised and cruciate retaining designs in the amount of ICIC on internal edges ($p = 0.0375$). This corrosion pattern was prevalent in our series of knee retrievals and may help explain some of the mechanisms of material loss that may occur *in vivo*.

Keywords: corrosion, knee prosthesis, CoCr, cell, inflammation

Running Heads: Inflammatory Cell Induced Corrosion in Total Knee Arthroplasty: A Retrieval Study

Introduction

Metals are widely used in orthopaedic implants due to their favourable mechanical properties and biocompatibility¹⁻². Numerous studies have reported evidence of metal release in patients

with joint replacements leading to local tissue reactions, pain and ultimately revision of the implant.³⁻⁹ The mechanisms of metal loss are multifactorial and can include mechanically assisted crevice corrosion (MACC), wear at the bearing surfaces and the recently described phenomenon of inflammatory cell induced corrosion (ICIC)^{8,9,12}.

Gilbert et al.⁸ and Di Laura et al.⁹ previously found evidence of inflammatory cell induced corrosion on CoCr retrieved implants and hypothesised that different classes of cells from both the skeletal and immune systems (such as phagocytic cells, osteoclasts, macrophages, foreign giant cells and polymorphonuclear leucocytes) may directly attack surfaces of metal implants, creating a unique damage pattern that is usually found on the non-contacting regions of retrieved components. This hypothesis is supported by *in vitro* studies^{10,11} showing that monocytes can differentiate into osteoclasts and corrode metallic surfaces made of titanium and stainless steel.

Kurtz et al.¹² recently investigated the phenomenon of ICIC in femoral components of total knee arthroplasty (TKA), however the extent and clinical relevance of this corrosion mechanism is not fully understood. In this study, we investigated the phenomenon of inflammatory cell induced corrosion in both femoral and tibial CoCr components of TKA, trying to understand in depth its clinical relevance through retrieval analyses. We aimed to:

- (1) identify the extent and location of ICIC patterns on our retrieved metallic components and
- (2) correlate our findings with implant and clinical information.

Methods

Our series of implants consisted of 28 total knee replacements, revised from 15 male and 13 female patients with a median (range) age of 65 (46-81) years and a median time to revision

of 36 (1-240) months; the designs consisted of 9 posterior stabilized (PS) and 19 cruciate retaining (CR) knees. The reasons for revision, as reported by the revising surgeon, were instability (n=10), aseptic loosening (n=5), infection (n=2), patella maltracking (n=2), unexplained pain (n=2), fracture (n=2), malposition (n=2), nickel allergy (n=1) and recurrent dislocation (n=1). Implant and patient demographics are summarised in Table 1.

In this study we focused our analysis on the polished CoCr components, using similar methods to those described by Gilbert⁸ and Di Laura⁹. We analysed 28 femoral components and 9 polished tibial plates.

Sample Preparation

All implants were decontaminated using 10% formaldehyde solution followed by soaking in 10% solution of Decon 90 in an ultrasonic cleaning bath for 30 minutes, and subsequent rinsing in distilled water and left to air dry¹⁴.

Macroscopic assessment and ICIC Localisation

All component surfaces were visually divided into different sections, in order to localise areas of ICI corrosion damage. The polished surfaces of the femoral components were divided into 9 sections, Figure 1. The sub-division was made to differentiate between the articulating regions and those which are not designed to be in contact with other component surfaces. The flexion and extension lateral and medial condyles were considered as being normally contacting regions whilst the internal and external edges, the trochlea and the lateral and medial trochlear compartments were considered as not normally articulating or being in limited contact.

The tibial components were divided into 9 sections, Figure 2 A-B, in order to distinguish between areas covered by the polyethylene tibial insert (internal sections) and areas not

covered (external sections).

All the components were analysed macroscopically and with the aid of a Keyence VHX-700F series (Keyence Co., Japan) digital microscope in order to assess the presence and localisation of cell induced corrosion, using magnifications up to 1000X.

In digital optical microscopic images, the patterns of cell induced corrosion appear as light frosted or discoloured areas.

ICIC Quantification

In order to accurately quantify the dimensions of the area covered by ICIC, we used the same photogrammetric method described by Di Laura et al.;⁹ pictures of the zones of interest were taken with an imaging system (EOS 5D Mark II camera, Canon, Tokyo, Japan) and subsequently analysed with a public domain software tool (ImageJ 1.4.3.6.7, Broken Symmetry Software). Image calibration was performed using a reference scale in the field of view.

SEM and EDS analyses

Detail microscopic analysis of areas of interest highlighted during the macroscopic assessment was performed using a Scanning Electron Microscope SEM (Jeol JSM5500, Tokyo, Japan). This imaging modality allows the identification of individual fine pits and circular or irregular crater-like features that are characteristic of ICIC.

Both high (10-20) kV Second Electron Imaging (SEI) and high (10-15) kV Backscattering imaging (BEC) were used: high energy electron beams can pass mostly through biological materials with few scattered electrons providing image contrast. SEI provides topographic information about the alloy, while high voltages BEC can also give clues about the composition of the surface. Energy Dispersive X-ray Spectrometry (EDS) was also performed

in order to investigate the elemental composition of deposits from biocorrosion on the implant surface.

Wear assessment on polyethylene articular surfaces

The tibial polyethylene inserts were forensically analysed using a Keyence VHX-700F series (Keyence Co., Japan) digital microscope, with magnification from 50X up to 200X. Each of the 28 polyethylene articular surfaces were divided into 10 sections and analysed using the Hood score, according to the presence and severity of seven modes of surface degradation (surface deformation, pitting, embedded debris, scratching, burnishing, abrasion and delamination)¹³. The maximum total damage grade was 210 (grade 3 for each of the seven damage modes for each of the 10 sections). Grading was performed by two different examiners; in case of disagreement, the examiners discussed the results together, in order to agree a final grade.

Statistical Analysis

Non parametric Spearman two-tailed tests (CI 95%) were performed using Prism 7 (GraphPad, USA) in order to investigate any correlations between both the presence and the extent (the total amount of area covered by corrosion) of ICIC corrosion and implant and clinical variables; P values <0.05 were considered significant. Moreover, we performed unpaired non parametric tests (Mann-Whitney test) in order to identify any significant difference in the extent of ICIC between PS and CR designs and between cemented and uncemented implants; P values <0.05 were considered significant.

Results

ICIC Localisation and Quantification

Our results revealed that 71% (n=20) of the femoral and 100% (n=9) of tibial components respectively showed presence of cell induced corrosion. The mean (range) cumulative area with ICIC damage on the femoral components was 40.04 (1.72-99.35) mm², while the tibial one was 57.94 (7.95-129.81) mm². The surface regions with evidence of ICIC made up approximately 1% and 2% of the entire surface areas of the femoral and tibial components respectively. We identified discoloured and light frosted zones, Figure 3, which at higher magnifications were found to be pits and crater-like spots, Figure 4.

Figure 5 shows the distribution of ICIC across the femoral component surfaces; 38% of these corrosion patterns were localised to the trochlea region and internal edges on the femoral components, whilst 28% was found across the lateral and medial external edges. The lateral and medial trochlear regions had the 9% and 12% respectively, while the remaining sections showed less than 5% each. The mean surface area of ICIC for non-contacting zones was 4.13 mm², whilst for contact zones it was 0.96 mm²; this difference was significant (p<0.0001). On the tibial component, 89% of the ICIC damage was found on the edge and the external sections, while 11% on the internal ones, Figure 6; the difference between external (mean value= 11.73 mm²) and internal (mean value= 1.85 mm²) zones was also significant (p<0.0001).

SEM and EDS analyses

SEM images confirmed our findings from our previous visual assessment: Figure 7 demonstrates the light frosted and discoloured areas high magnification. We identified the fine biologically-derived corrosion patterns described by Gilbert et al.⁸: the macroscopically hazy regions revealed to consist of an extension of pits, in the order of 10 µm, and craters with ruffled borders (Figure 7 A, B). Examples of suspected single cell attacks are also shown with central, flat and smooth ovals surrounded by concentric rings; this pattern reflects a

typical cell structure (Figure 7 C, red arrows). Moreover, it is also possible to appreciate the characteristic pattern of migrating cells (Figure 7 D, red arrow) which left a streak of corrosion after their surface attack. Figure 8 shows both the high voltage SEI (A) and high voltage BEC (B) images: in the first case biological material appear as a bright spot in the middle of a crater, while the metallic surface underneath is highlighted using in the backscattering image. EDS analyses detected the presence of iron only in areas corresponding to corroded metallic surface (Figure 9).

Wear assessment on polyethylene articular surfaces

We found that the most common types of surface damage were burnishing, pitting and scratching. The mean Hood Score total value was 46, with a range of 21-61.

Statistical Analysis

Statistical analysis revealed no significant correlation between the extent of ICI corrosion and patient age, gender, time of implantation and reason for revision. Moreover, we did not find any significant correlation between ICIC extent and wear on polyethylene tibial inserts, Table 2.

We found a significant association between the presence of ICIC in femoral components and instability ($p=0.0113$), whilst there was no significant correlation between ICIC and the other reasons for revision, Table 3.

We did not find any significant difference in the extent of ICIC between PS and CR designs and between cemented and uncemented implants, Table 4. However, we found that posterior stabilized designs showed no cell induced corrosion in the internal femoral edges, while in the same section of cruciate retaining designs we did see this corrosion pattern with a mean value of 8.13 mm^2 ; this difference was significant ($p=0.0375$).

Discussion

The concerns about metal ions release in patients with joint replacements is highly topical following findings of adverse reactions in the local tissues surrounding implants at revision surgery¹⁻⁴. Several processes may generate this response and inflammatory cell induced corrosion is speculated to be one of them. Although this corrosive mechanism has been widely investigated in total hip replacements, there are few studies in total knee replacement: Gilbert⁸ and Kurtz¹² analysed retrieved femoral components only in their work on ICIC in failed TKRs.

We aimed to identify the extent and location of ICI corrosion on both femoral and tibial retrieved components and correlate our results with patient implant and clinical data. We found that 71% and 100% of femoral and tibial components respectively showed the surface changes described by Gilbert et al.⁸, thought to be inflammatory cell induced corrosion: this results differs from Kurtz's study, in which only 29% of femoral components showed evidence of ICIC¹². They also stated that the median cumulative area covered by ICIC was 0.07 mm², in contrast with our result of 25 mm²: they investigated only the bearing surface of the femoral component, which is thought to be a region poorly affected by ICIC presence. Our results showed that the major part of the damage was found on non-contact or less involved surfaces (87% and 89% in femoral and tibial components respectively), as indicated by previous papers^{8,9,12}; however only a maximum of 2% of the surfaces showed evidence of this corrosion mechanism.

We found no correlation between the amount of ICIC and both the implant and patient data; however, due to the presence of the peg which articulated with the cam, PS knee replacements showed no evidence of cell induced corrosion on the internal edges; in contrast, we did see evidence of ICIC in CR design which did not have this component (p<0.0001). This supports the hypothesis that the unique corrosive pattern may be caused by

inflammatory cells, that attack the non-contacting areas. Furthermore, we found a significant correlation between presence of ICIC and instability ($p=0.0113$); Di Laura et al.⁹ found a relationship between presence of ICIC and aseptic loosening. This suggests that the occurrence of ICIC could be involved in changes of mechanical integrity of the bone-implant interface.

SEM and EDS analyses showed that the corrosive damage was consistent with what was described and found in previous studies^{8,9,12}: the light frosted and discoloured areas consisted in several streaks of pits and crater-like features and different types of corrosion patterns were identified. The dimensions of the pits were around 10-20 μm and their pattern reflected the cell structure, and supports Gilbert's findings. Furthermore, iron was found in the corroded zones: this element is a fundamental component of phagocytic cells and it is known to be involved in inflammatory events. This supports the hypothesis that this damaged may be caused by cells involved in the inflammatory response.

In this study we analysed 28 femoral components and 9 tibial trays, and found evidence of inflammatory cell induced corrosion in 71% and 100% of the implants respectively. The majority of corroded areas (87% and 89% in femoral and tibial components respectively) were found in the non-articulating regions and the presence of ICI corrosion on the femoral components appeared to have a significant correlation with instability. This corrosion pattern was prevalent in our series of knee retrievals and may help explain some of the material loss that may occur *in vivo*. ICIC may help to explain failure in some cases, however only a maximum of 2% of the total surfaces was affected by this unique corrosion pattern and further work is required to determine the clinical significance of this corrosion mechanism.

Acknowledgments

The authors are grateful for the support of Dr. Michael Hirschmann, Dr. Paul Allen and Dr.

Martyn Porter for contributing their implants to our retrieval collection.

References

1. Jacobs JJ, Gilbert JL, Urban RM. Current Concepts Review-Corrosion of Metal Orthopaedic Implants. *The Journal of Bone & Joint Surgery* 80(2): 268,1998
2. Black J. Requirement for successful total knee replacement. Material consideration. *The Orthopaedic clinics of North Maerica* 20(1): 1, 1989
3. Caicedo MS, Pennekamp PH, McAllister K, Jacobs JJ, Hallab NJ. Soluble ions more than particulate cobalt-alloy implant debris induce monocyte costimulatory molecule expression and release of profinflammatory cytokines critical to metla-induced lymphocyte reactivity. *J Biomed Mater Res Part A*. 2010;93:1312-1321
4. Natu S, Sidaginamale RP, Gandhi J, Langton DJ, Nargol DJ, Antoni VF. Adeverse reaction to metal debris: histopathological features of periprosthetic soft tissue reactions seen in association with failed metal on metal hip arthroplasties. *J Clinic Path*. 2012; Vol 65(No 5): 409-418
5. Davies AP, Willert HG, Campbell PA, Learmonth ID, Case CP. An unusual lymphocytic perivascular infiltration in tissues around contemporary metal-on-metal joint replacements. *J Bone Joint Surg Am*. 2005;87:18–27
6. Lee SH, Brennan FR, Jocabos JJ, Urban RM, Ragasa DR, Glant TT. Human monocyte/macrophage response to cobalt-chromium corrosion products and titanium particles in patients with total joint replacements. *J Orthop Res*. 1997 Jan;15(1):40-9

7. Lassus J, Jiranek WA, Santavirta S, Nevalainen J, Mattucci-Cerinic M, Horák P, Konttinen Y. Macrophage activation results in bone resorption. *Clin Orthop Relat Res*. 1998 Jul;(352):7-15
8. Gilbert JL, Sivan S, Liu Y, Kocagöz SB, Arnholt CM, Kurtz SM. Direct in vivo inflammatory cell-induced corrosion of CoCrMo alloy orthopedic implant surfaces. *J Biomed Mater Res A*. 2015 Jan;103(1):211-23
9. Di Laura A, Hothi HS, Meswania JM, Whittaker RK, de Villiers D, Zustin J, Blunn GW, Skinner JA, Hart AJ. Clinical relevance of corrosion patterns attributed to inflammatory cell-induced corrosion: A retrieval study. *J Biomed Mater Res B Appl Biomater*. 2015 Oct 6
10. Cadosch D, Al-Mushaiqri MS, Gautschi OP, Meagher J, Simmen HP, Filgueira L. Biocorrosion and uptake of titanium by human osteoclasts. *J Biomed Mater Res A*. 2010 Dec 15;95(4):1004-10
11. Cadosch D, Chan E, Gatuschi OP, Simmen HP, Filgueira L. Bio-corrosion of stainless steel by osteoclasts--in vitro evidence. *J Orthop Res*. 2009 Jul;27(7):841-6
12. Arnholt CM, MacDonald DW, Malkani AL, Klein GR, Rimnac CM, Kurtz SM. Corrosion Damage and Wear Mechanism in Long-Term Retrieved CoCr Femoral Components for Total Knee Arthroplasty, *The Journal of Arthroplasty* (2016)
13. Hood RW, Wright TM, Burstein AH. Retrieval analysis of total knee prostheses: A method and its application to 48 total condylar prostheses. *J. Biomed. Mater. Res*. 1983, 17: 829–842.

Figures

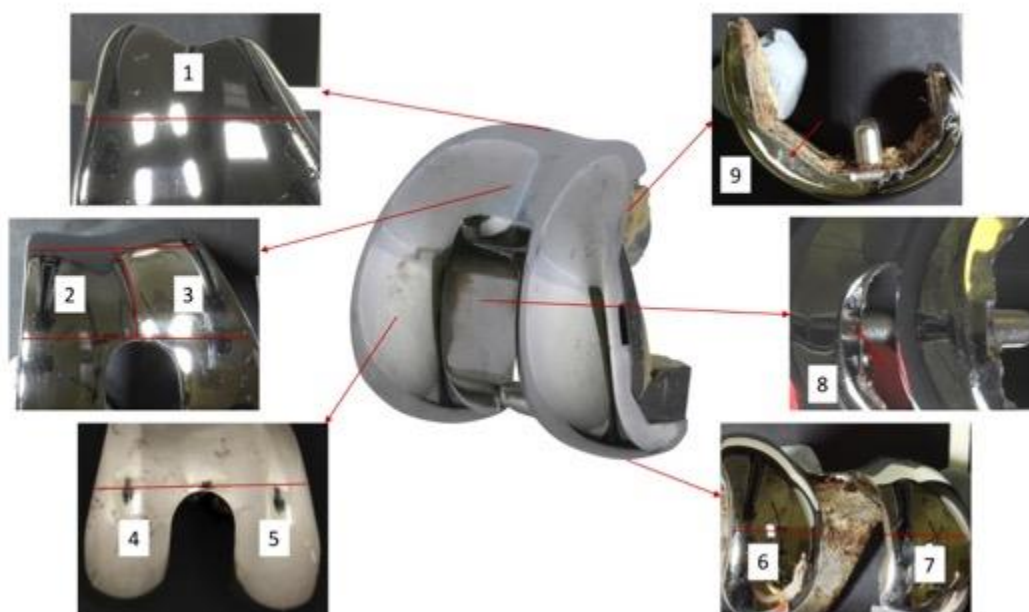


Figure 1: Sub-division of the femoral component in 9 sections. (1) trochlea; (2) lateral and (3) medial trochlear compartments; (4) extension lateral and (5) medial condyles; (6) flexion lateral and (7) medial condyles; (8) internal and (9) external edges. This division was performed according to the differentiation between the articulating regions (4, 5, 6, 7) and those which are not designed to be in contact with other component surfaces (1, 2, 3, 8, 9).

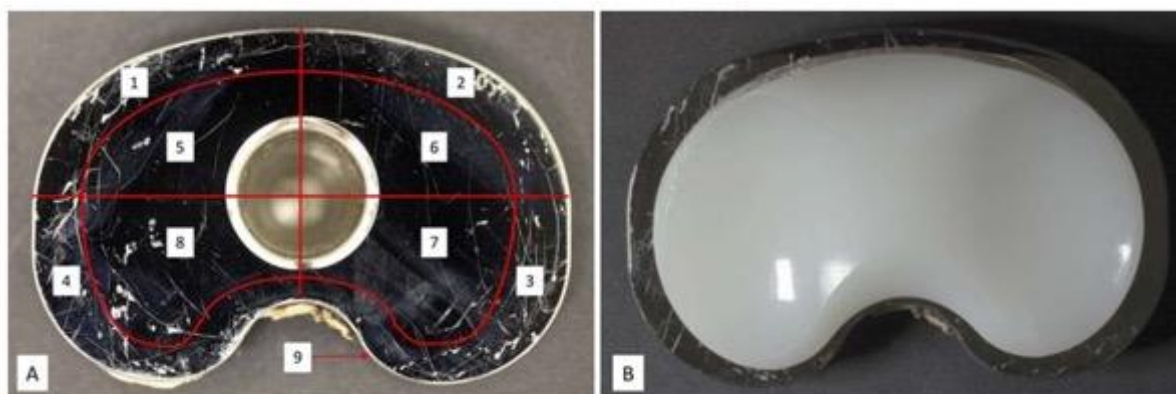


Figure 2: (A) Sub-division of the tibial component in 9 sections. (1) external medial anterior section; (2) external lateral anterior section; (3) external lateral posterior section; (4) external medial posterior section; (5) internal medial anterior section; (6) internal lateral anterior section; (7) internal lateral posterior section; (8) internal medial posterior section; (9) edge. (B) This division was performed in order to distinguish between areas covered by the polyethylene tibial insert (internal sections) and areas not covered (external sections).

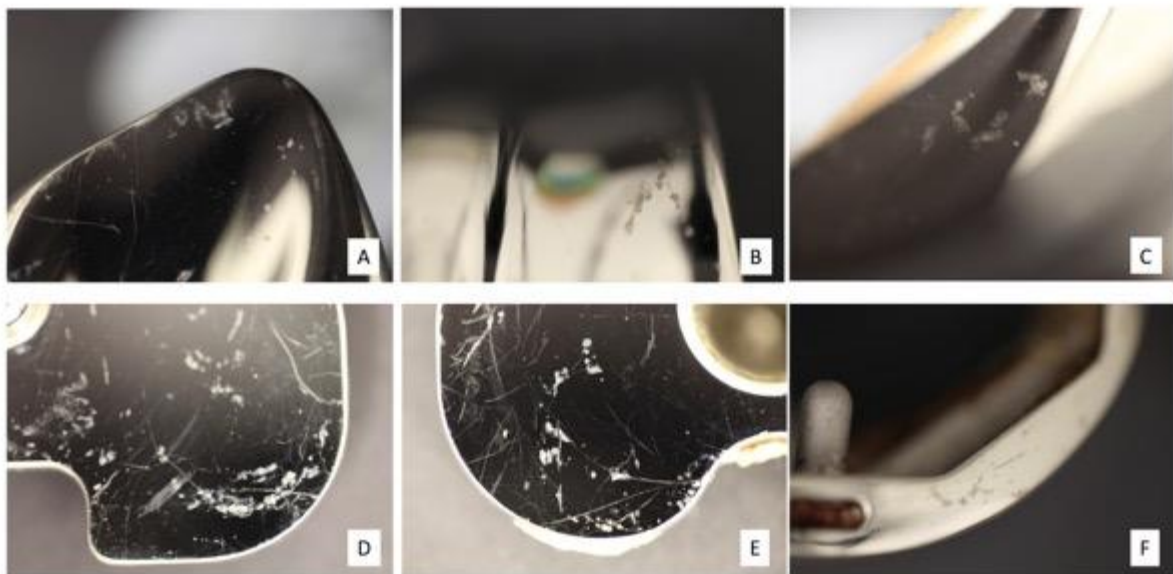


Figure 3: Pictures taken with an imaging system (EOS 5D Mark II camera, Canon, Tokyo, Japan) showing discoloured and light frosted regions identified on different surfaces. (A) trochlea; (B) medial trochlear compartment; (C) external edge; (D-E) tibial components; (F) external edge.

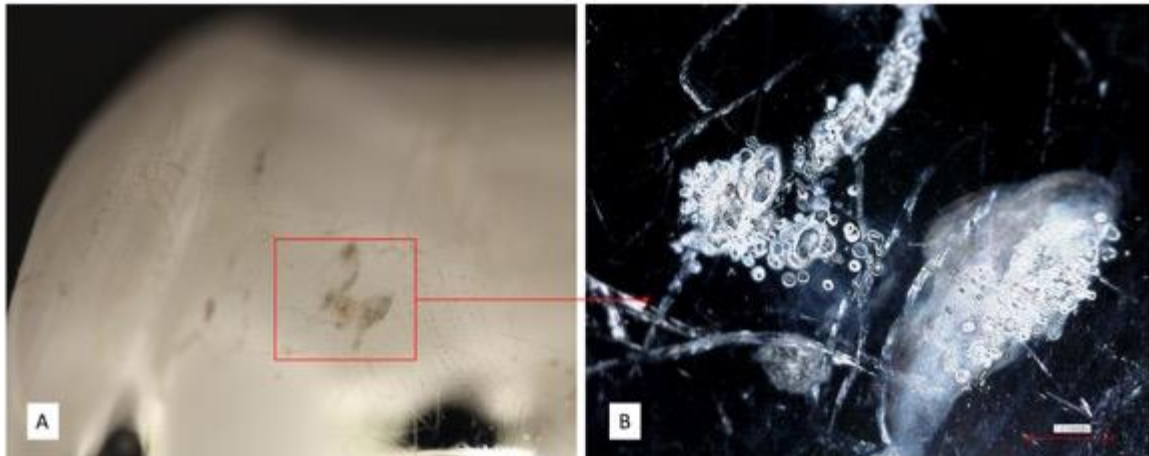


Figure 4: (A) Picture taken with an imaging system (EOS 5D Mark II camera, Canon, Tokyo, Japan) showing a discoloured and light frosted area. (B) The same area visually analysed by a digital microscope with magnification X100: this zone is composed pits and crater-like spots.

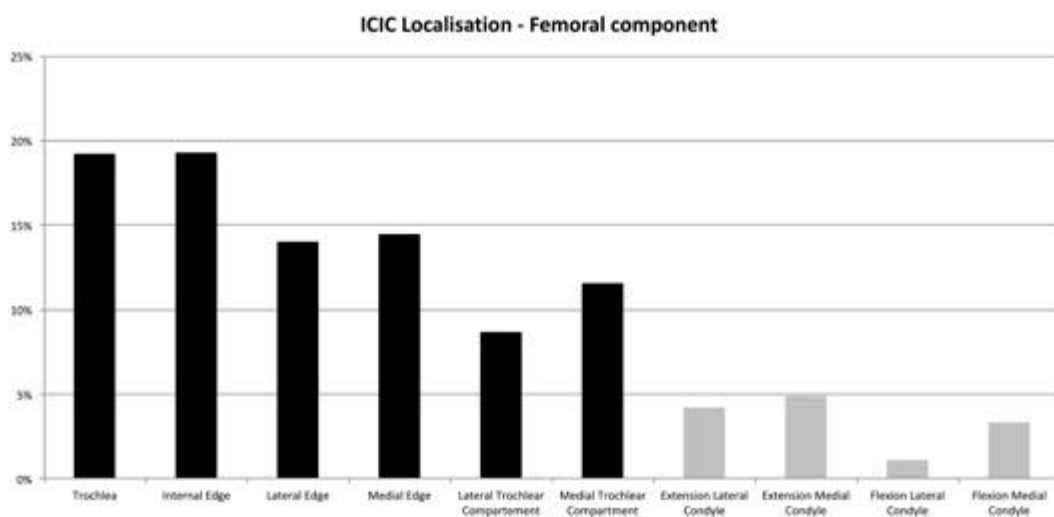


Figure 5: Bar graph showing the localisation (in percentage) of ICIC on femoral component. The non-contacting (black bars) and contact (grey bars) zones are highlighted.

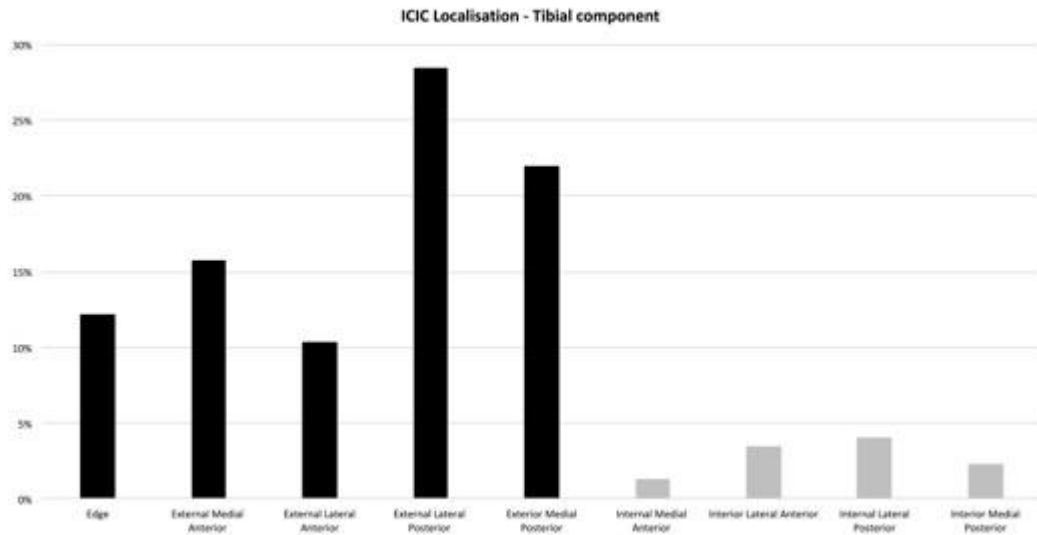


Figure 6: Bar graph showing the localisation (in percentage) of ICIC on tibial component. The external (black bars) and internal (grey bars) zones are highlighted.

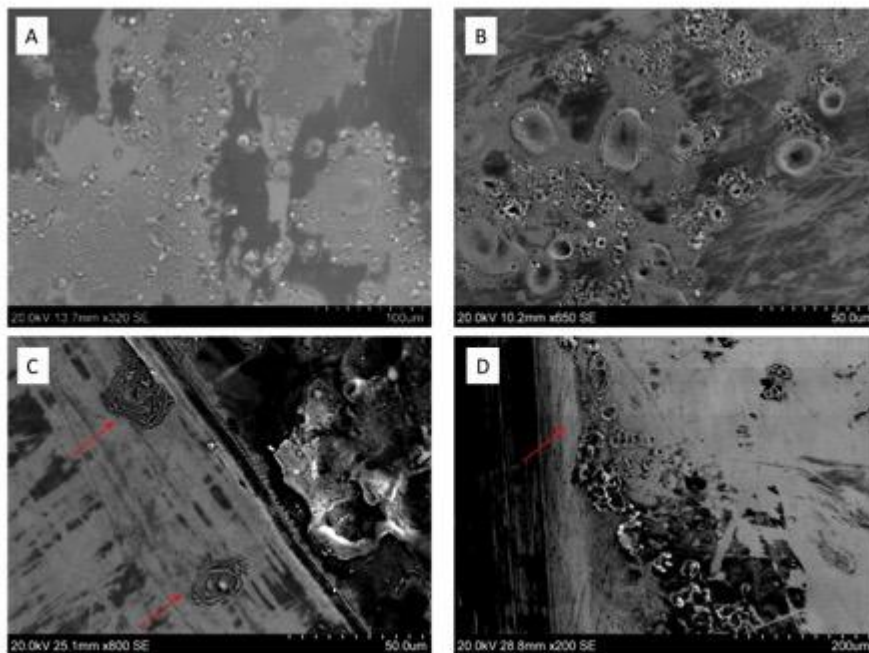


Figure 7: Pictures taken, using a scanning electron microscope, illustrating the biologically-derived corrosion pattern at high voltage (20 kV) and different magnifications (from X200 up to X800). (A,B) Extension of pits and crater-like features; (C) example of suspected single cell attack which consists in a region with a central, flat and smooth oval surrounded by concentric rings (red arrows); (D) unique corroded pattern suspected due to cells migration.

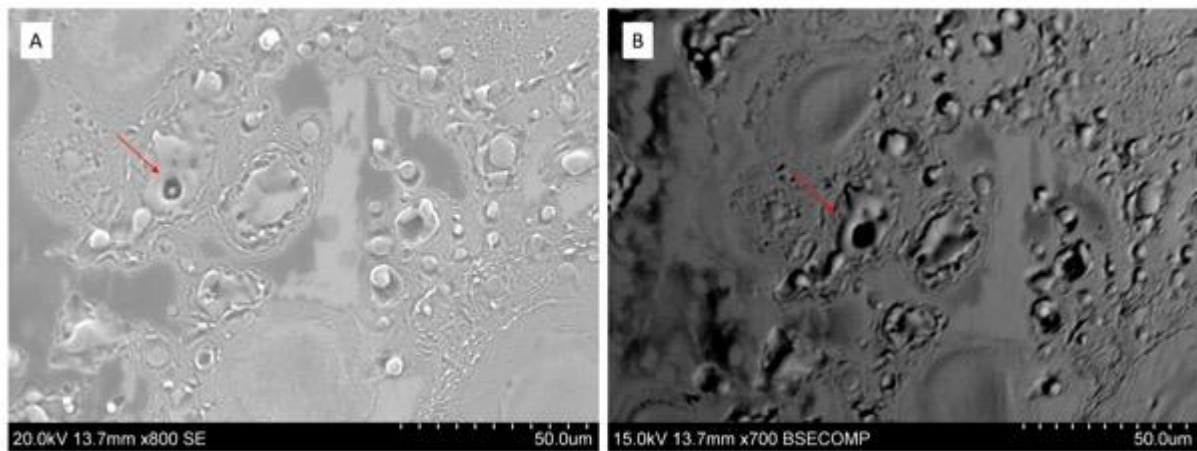


Figure 8: Image showing the difference between two scanning mode: (A) Second Electron Imaging SEI and (B) Backscattering imaging BEC. It is possible to notice that SEI highlights biological material (bright spot) in the corroded region, whilst BEC shows the metal surface of the alloy underneath the biological residue.

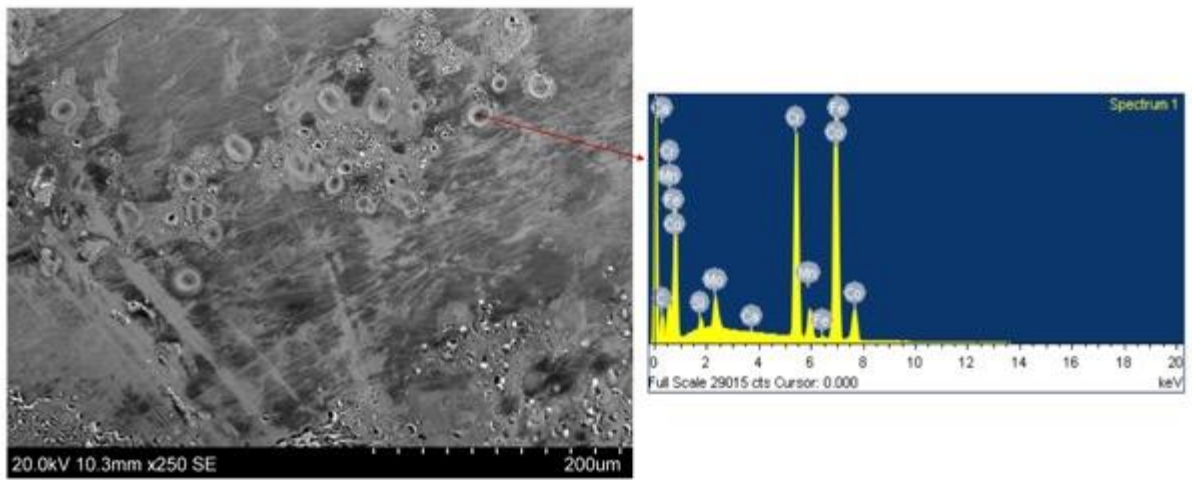


Figure 9: EDX image showing the elemental composition in a corroded area (red arrow). The spectrum identified the presence of Fe, which presumably derived from Feantion-like reactions involving reactive oxygen species.

	Implant				Patient		
Case Number	Components	Design	Bone Interface	Implantation time [months]	Reason for revision	Age [years]	Gender

1	Femoral	PS	Cemented	29	Infection	69	M
2	Femoral	CR	Uncemented	72	Instability	65	F
3	Femoral	CR	Cemented	15	Aseptic loosening	69	M
4	Femoral and Tibial	CR	Uncemented	53	Malposition	66	M
5	Femoral	PS	Cemented	72	Instability	53	F
6	Femoral and Tibial	CR	Uncemented	36	Instability	69	M
7	Femoral	PS	Cemented	96	Aseptic loosening	75	M
8	Femoral and Tibial	CR	Cemented	72	Instability	66	M
9	Femoral and Tibial	CR	Cemented	40	Patella maltracking	61	F
10	Femoral	PS	Cemented	27	Not available	76	M
11	Femoral	CR	Cemented	Not available	Patella maltracking	78	F
12	Femoral and Tibial	CR	Uncemented	20	Pain	46	F
13	Femoral	CR	Cemented	10	Instability	62	M
14	Femoral	PS	Cemented	36	Loosening	61	M
15	Femoral and Tibial	CR	Cemented	120	Instability	49	M
16	Femoral	CR	Cemented	240	Loosening	56	F
17	Femoral	CR	Cemented	< 1	Recurrent Dislocation	74	F
18	Femoral	CR	Cemented	85	Instability	81	F
19	Femoral	CR	Cemented	53	Infection	65	M
20	Femoral and Tibial	PS	Uncemented	10	Malposition	64	M

21	Femoral	PS	Cemented	Not available	Fracture	Not available	M
22	Femoral	CR	Cemented	72	Nickel allergy	67	F
23	Femoral	CR	Cemented	144	Fracture	69	F
24	Femoral	CR	Uncemented	33	Aseptic loosening	72	F
25	Femoral	PS	Cemented	5	Pain	51	F
26	Femoral and Tibial	CR	Uncemented	22	Instability	51	M
27	Femoral and Tibial	CR	Uncemented	24	Instability	71	F
28	Femoral	PS	Cemented	36	Instability	48	M

Table 1: Implant and patient demographics.

	ICIC Extent						
	Patient information			Reason for revision			Wear on polyethylene tibial inserts
	Age	Gender	Time of implantation	Instability	Aseptic loosening	Infection	
Femur	NO p=0.1571	NO p=0.2294	NO p=0.5697	NO p=0.3542	NO p=0.2909	NO p=0.4908	NO p=0.9890
Tibia	NO p=0.2698	NO p=0.1908	NO p=0.1081	NO p=0.1265	*	*	NO p=0.2745

Table 2: Results from statistical analysis about the correlation between extent (calculated as total amount of area covered by corrosion, in mm²) of ICIC and implant (reason for revision, wear on polyethylene) and patient (age, gender and time of implantation) demographic, showing p values, for both femur and tibia.

* insufficient numbers available for statistical analysis

	ICIC Presence					
	Patient information			Reason for revision		
	Age	Gender	Time of implantation	Instability	Aseptic loosening	Infection
Femur	NO* p=0.2730	NO p=0.8190	NO* p=0.2061	YES p=0.0113	NO p=0.0922	NO p=0.5046
Tibia	**	**	**	**	**	**

Table 3: Results from statistical analysis about the correlation between presence of ICIC and implant (reason for revision) and patient (age, gender and time of implantation), showing p values, for both femur and tibia.

* We investigated the presence of significant differences between implants with presence of ICIC and those with no evidence of it.

** It was not possible to evaluate the correlation between the ICIC presence and any variables because the 100% of tibial implants showed cell induced corrosion

	Difference in the ICIC extent	
	Design (PS v CR)	Fixation method (cemented vs uncemented)
Femur	NO p=0.1934	NO p=0.0510
Tibia	NO p=0.2023	NO p=0.3793

Table 4: Results from statistical analysis investigating significant differences in ICIC extent between extent implants designs (PS vs CR) and fixation methods (cemented vs uncemented), showing p values are shown, for both femur and tibia.